Analysis of Radiative Equilibrium in a Rectangular Enclosure With Gray Medium

W. W. Yuen

L. W. Wong[1]

Department of Mechanical and Environmental Engineering, University of California, Santa Barbara, Calif. 93106

Radiative heat transfer and temperature profile in a two-dimensional rectangular enclosure with gray medium are calculated. Successive approximate solutions are generated by a point allocation method in which the temperature profile is expressed as polynomials of successively higher order. The technique is shown to converge rapidly with the third-order results already comparing favorably with available numerical solution. It is also demonstrated to be computationally efficient. Comparing with a solution with the same number of unknowns generated by the Hottel zonal method, the present approach represents a reduction in computational time by at least one order of magnitude. Based on the mathematical behavior of the numerical results, simple empirical closed-form approximate expressions for both the heat transfer and temperature profile in general multidimensional systems at radiative equilibrium are proposed. For a rectangular enclosure, these expressions are demonstrated to be quite accurate over all optical thickness.

1 Introduction

Radiative heat transfer in an absorbing and emitting medium constitutes an important element in many engineering disciplines. A great deal of work has been reported in this area. Most, however, has been confined to one-dimensional systems, largely due to the complexity of the problem. Over the past decade, there has been a considerable increase in the interest of multidimensional radiative transfer. Different numerical techniques [1,2] and approximation methods [3–5] have been developed for some selected cases. But the success of these works, in terms of their applicability to radiative transfer in general multidimensional systems, is still quite limited.

Numerically, both the Monte Carlo method [1] and the Hottel zonal method [2] have been widely used for multidimensional computations. But results of the computation generally show that these methods can be quite time consuming and inaccurate under certain conditions. Without significant improvements, it appears unlikely that these two methods can be effectively applied for predicting radiative heat transfer in practical engineering systems.

For approximate analysis, the most successful technique for multidimensional radiative transfer appears to be the modified differential approximation. Based on this method, Glatt and Olfe [3] calculated the temperature distribution in a gray medium bounded by a black rectangular enclosure. Utilizing essentially the same technique and aided by the introduction of a number of geometric parameters, Modest [4, 5] obtained solutions not only for a rectangular enclosure with gray walls, but also for a two-dimensional problem with cylindrical symmetry. But both of these approaches require extensive numerical computation for their prediction of temperature distribution and heat flux. It also appears difficult, if not impossible, to apply these methods for systems with arbitrary geometry. The value of any approximation method depends on its simplicity, accuracy, and applicability to general systems. None of the existing approximation methods appears to have all of these qualities.

The objective of the present work is twofold. First, the point allocation method, which was successful in generating accurate solutions to one-dimensional radiative transfer problems even including the effect of conduction and anisotropic scattering [6, 7], will be demonstrated to be applicable for two-dimensional problems. A gray medium bounded by a rectangular enclosure at radiative equilibrium is analyzed as an illustration. By expanding the unknown temperature distribution as a polynomial, the governing integral equation is reduced to a set of algebraic equations in terms of the expansion coefficients. Successive solutions with increasing degree of accuracy can be readily generated. Comparing with the Hottel zonal method, the present approach is both accurate and efficient. The third-order solution, which involves 28 unknown expansion coefficients, already compares favorably with the available numerical results. This rapid rate of convergence appears to hold for all optical thicknesses and aspect ratios of the rectangular enclosure. By expressing elements of the resulting matrix equation in terms of a class of generalized exponential integral functions which was studied extensively in a recent work [8], the present solution method is extremely efficient numerically. All solutions are generated by evaluating a finite number of single integrations and a matrix inversion. The number of single integrals required is approximately the same as the number of double integrals required for a Hottel zonal calculation with the same number of unknowns.

The second objective of the present work is to develop simple closed-form approximate expressions for the prediction of radiative heat transfer and temperature profile in a gray medium at radiative equilibrium within a general multidimensional enclosure. By requiring that the approximation yield the correct result both in the optically thick and thin limits, a generalized diffusion approximation is proposed. For the present rectangular enclosure, the accuracy of the approximation is shown to be quite good.

2 Mathematical Formulation

The physical model and its associated coordinate system is shown in Fig. 1. For simplicity, the four boundaries are assumed to be black isothermal surface with normalized

[1] Now with The Xerox Corporation, Redondo Beach, Calif.

Contributed by the Heat Transfer Division for publication in the JOURNAL OF HEAT TRANSFER. Manuscript received by the Heat Transfer Division September 16, 1982.

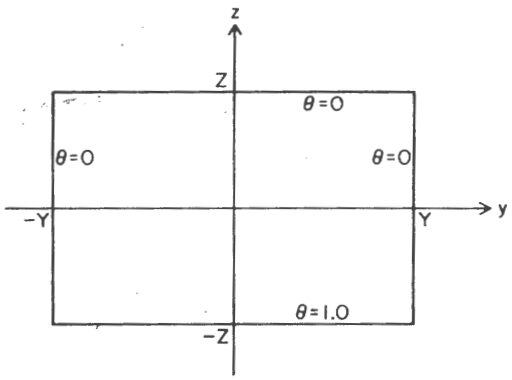

Fig. 1 Geometry and coordinate system for the two-dimensional rectangular enclosure

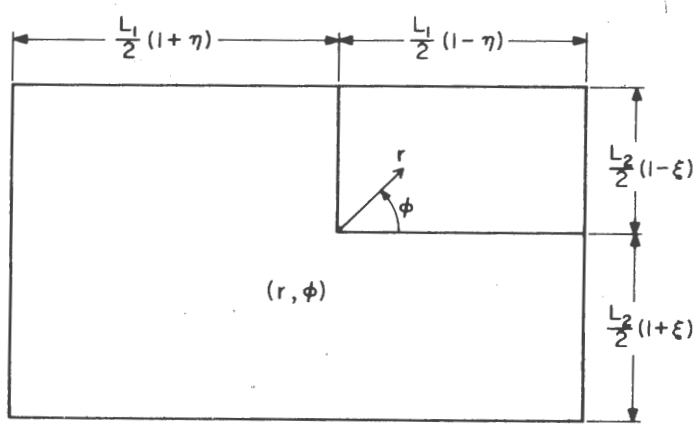

Fig. 2 Domain of integration used in equations (13-15)

emissive powers of 1, 0, 0, and 0, respectively. From standard reference [9], the energy equation for the medium at radiative equilibrium is given by

$$4\vartheta(\mathbf{r}) = \int_{\partial V} \frac{\mathbf{n}(\mathbf{r}')(\mathbf{r}-\mathbf{r}')}{\pi|\mathbf{r}-\mathbf{r}'|^3} C(\mathbf{r}-\mathbf{r}')dS + \int_V \vartheta(\mathbf{r}'') \frac{e^{-a|\mathbf{r}-\mathbf{r}''|}}{\pi|\mathbf{r}-\mathbf{r}''|^2} adV \tag{1}$$

where $\vartheta(\mathbf{r}) = \sigma T^4(\mathbf{r})$ is the blackbody emissive power; $\mathbf{r}'$, a point located at the boundary and $\mathbf{n}(\mathbf{r}')$ the corresponding unit normal vector; a, the absorption coefficient which for the present work is assumed to be constant; and $C(\mathbf{r}-\mathbf{r}')$, a function given by

$$C(\mathbf{r}-\mathbf{r}') = \begin{cases} e^{-a|\mathbf{r}-\mathbf{r}'|} & z' = -Z \\ 0 & \text{otherwise} \end{cases} \tag{2}$$

The medium's temperature is determined by solution to equation (1). Once the temperature distribution is determined, the radiative heat flux is given by

$$\mathbf{Q}(\mathbf{r}) = \int_{\partial V} \frac{\mathbf{n}(\mathbf{r}')(\mathbf{r}-\mathbf{r}')}{\pi|\mathbf{r}-\mathbf{r}'|^4} C(\mathbf{r}-\mathbf{r}')(\mathbf{r}-\mathbf{r}')dS + \int_V \vartheta(\mathbf{r}'') \frac{e^{-a|\mathbf{r}-\mathbf{r}''|}}{\pi|\mathbf{r}-\mathbf{r}''|^3} a(\mathbf{r}-\mathbf{r}'')dV \tag{3}$$

For the present two-dimensional problem, all integrals in the x-direction can be integrated. Introducing the following dimensionless variables

$$\eta = \frac{y}{Y} \tag{4}$$

$$\zeta = \frac{z}{Z}$$

$$L_1 = 2aY$$

$$L_2 = 2aZ,$$

equations (1) and (3) can be simplified to yield

$$\vartheta(\eta,\zeta) = \frac{L_1L_2}{16}\int_{-1}^{1}\int_{-1}^{1} \vartheta(\eta',\zeta')\frac{S_1(d_1)}{d_1}d\eta'd\zeta' + \frac{L_1L_2}{16}(1+\zeta)\int_{-1}^{1}\frac{S_2(d_2)}{d_2^2}d\eta' \tag{5}$$

$$Q_\eta(\eta,\zeta) = \frac{L_1^2L_2}{8}\int_{-1}^{1}\int_{-1}^{1} \vartheta(\eta',\zeta')\frac{S_2(d_1)(\eta-\eta')}{d_1^2} \tag{6}$$

$$d\eta'd\zeta' + \frac{L_1^2L_2}{8}(1+\zeta)\int_{-1}^{1}\frac{S_3(d_2)(\eta-\eta')}{d_2^3}d\eta'$$

$$Q_\zeta(\eta,\zeta) = \frac{L_1L_2^2}{8}\int_{-1}^{1}\int_{-1}^{1} \vartheta(\eta',\zeta')\frac{S_2(d_1)(\zeta-\zeta')}{d_1^2} \tag{7}$$

$$d\eta'd\zeta' + \frac{L_1L_2^2}{8}(1+\zeta)^2\int_{-1}^{1}\frac{S_3(d_2)}{d_2^3}d\eta'$$

Nomenclature

a = absorption coefficient
$C(\mathbf{r}-\mathbf{r}')$ = function defined by equation (2)
$d_1(\eta,\eta',\zeta,\zeta',)$ = function defined by equation (8)
$d_2(\eta,\eta',\zeta,)$ = function defined by equation (9)
$G_{m,n,k}(x,y)$ = function defined by equation (22)
$H_{m,n,k,s}(\eta,\zeta)$ = function defined by equations (A3) and (A4)
L_1 = optical thickness of the enclosure in the y-direction
L_2 = optical thickness of the enclosure in the z-direction
$M_{i,j}$ = function defined by equation (20)
$\mathbf{n}$ = unit normal vector
$NY_{i,j}$ = function defined by equation (27)
$NZ_{i,j}$ = function defined by equation (28)
$P_{i,j}$ = coefficients of assumed polynomial defined by equation (18)
Q_i = heat flux in the i-direction
$\mathbf{Q}$ = heat flux vector
r = "polar" coordinate defined by equations (11) and (12)
$\mathbf{r}$ = position vector
$S_n(x)$ = exponential integral function
T = temperature
$W_{m,n,k}(\eta,\zeta)$ = functions defined by equations (21)
x = coordinate
y = coordinate
z = coordinate
$\Gamma(n)$ = gamma function
ζ = optical thickness variable in the z-direction
η = optical thickness variable in the y-direction
ϑ = dimensionless emissive power
φ = angular coordinate defined by equations (11) and (12)
φ_1 = angle defined by equation (16)
φ_2 = angle defined by equation (17)
σ = Stefan-Boltzman constant

Subscripts

0 = optically thin limit
c = optically thick (conduction) limit

where

$$d_1(\eta,\eta',\zeta,\zeta') = \tfrac{1}{2}[L_1^2(\eta-\eta')^2 + L_2^2(\zeta-\zeta')^2]^{1/2} \tag{8}$$

$$d_2(\eta,\eta',\zeta) = d_1(\eta,\eta',\zeta,-1) \tag{9}$$

In equations (5), (6), and (7), $S_n(x)$ is a generalized exponential integral function defined by

$$S_n(x) = \frac{2}{\pi}\int_1^\infty \frac{e^{-xt}dt}{t^n(t^2-1)^{1/2}} \tag{10}$$

Analytical and numerical properties of $S_n(x)$ are presented in [8].

Since $S_n(x)$ is a smooth function for all values of x, evaluation of the integrals appearing in equations (5), (6), and (7) is quite straightforward for any assumed temperature distribution. Note that even at regions with $d_1=0$ or $d_2=0$, these integrals remain finite because the product of the integrand with the respective volume element and surface element remains finite. To illustrate this mathematical behavior more clearly and also for the convenience of numerical computation, equations (5-7) are now rewritten in terms of a "polar" coordinate. Introducing two new variables, r and φ, such that

$$\eta' = \eta + \frac{2r}{L_1}\cos\varphi \tag{11}$$

$$\zeta' = \zeta + \frac{2r}{L_2}\sin\varphi \tag{12}$$

equations (5), (6), and (7) can be rewritten as

$$4\vartheta(\eta,\zeta) = \int\int_{(r,\varphi)} \vartheta\left(\eta+\frac{2r}{L_1}\cos\varphi, \zeta+\frac{2r}{L_2}\sin\varphi\right) \tag{13}$$

$$S_1(r)drd\varphi + \int_{\varphi_1}^{\varphi_2} S_2\left[\frac{L_2}{2}(1+\zeta)\sec\varphi\right]d\varphi$$

$$Q_\eta(\eta,\zeta) = -\int\int_{(r,\varphi)} \vartheta\left(\eta+\frac{2r}{L_1}\cos\varphi, \zeta+\frac{2r}{L_2}\sin\varphi\right) \tag{14}$$

$$S_2(r)\cos\varphi drd\varphi - \int_{\varphi_1}^{\varphi_2} S_3\left[\frac{L_2}{2}(1+\zeta)\sec\varphi\right]\sin\varphi d\varphi$$

$$Q_\zeta(\eta,\zeta) = -\int\int_{(r,\varphi)} \vartheta\left((\eta+\frac{2r}{L_1}\cos\varphi, \zeta+\frac{2r}{L_2}\sin\varphi\right) \tag{15}$$

$$S_2(r)\sin\varphi drd\varphi + \int_{\varphi_1}^{\varphi_2} S_3\left[\frac{L_2}{2}(1+\zeta)\sec\varphi\right]\cos\varphi d\varphi$$

with

$$\varphi_1 = -\tan^{-1}\frac{L_1(1+\eta)}{L_2(1+\zeta)} \tag{16}$$

$$\varphi_2 = \tan^{-1}\frac{L_1(1-\eta)}{L_2(1+\zeta)} \tag{17}$$

The region of integration (r,φ) for the above double integration at a given (η,ζ) is illustrated by Fig. 2. Note that equations (13-15) are indeed free of any apparent singularites.

3 Method of Solution

The method of point allocation is now applied to develop solutions to the present problem. Specifically in the nth approximation, the unknown temperature distribution is assumed to be a polynomial as follows

$$\vartheta(\eta,\zeta) = \sum_{i=0}^{i=n}\sum_{j=0}^{j=2n} P_{2i,j}\eta^{2i}\zeta^j \tag{18}$$

Substituting equation (18) into equation (13), the following equation results

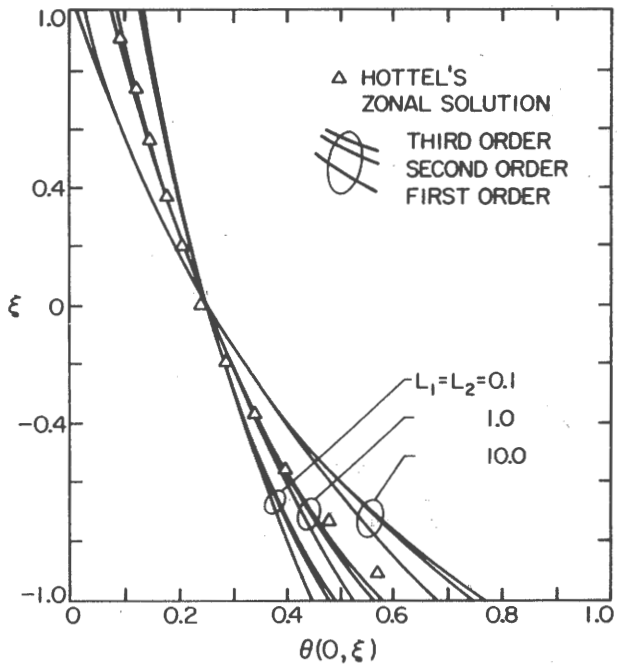

Fig. 3 Comparison between the first three order approximate temperature solutions with results generated by the Hottel's zonal method

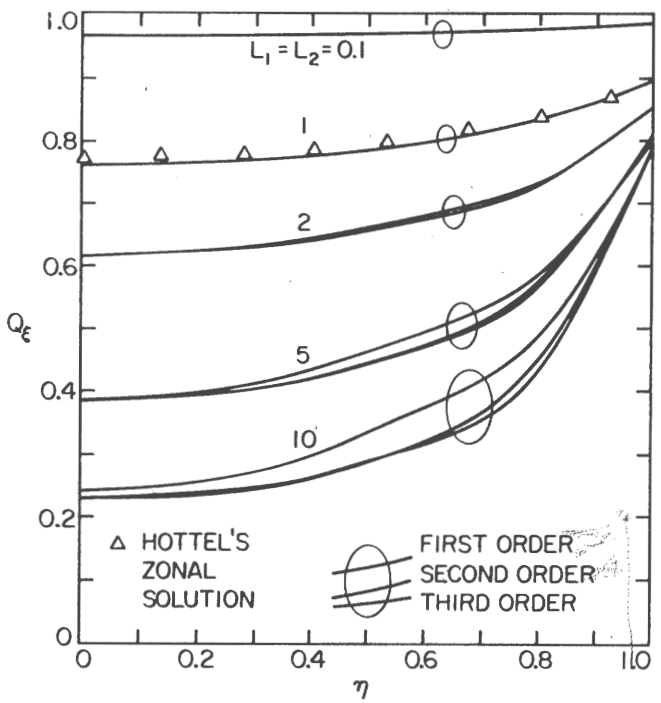

Fig. 4 Comparison between the first three order approximate heat flux solutions with results generated by the Hottel's zonal method

$$\sum_{i=0}^{i=n}\sum_{j=0}^{j=2n} P_{2i,j}[4\eta^{2i}\zeta^j - M_{2i,j}(\eta,\zeta,L_1,L_2)]$$

$$= G_{0,0,0}(\zeta^+,\eta^+) + G_{0,0,0}(\zeta^+,\eta^-) \tag{19}$$

where

$$M_{2i,j} = \sum_{mi=0}^{mi=2i}\sum_{ni=0}^{ni=j}\binom{2i}{mi}\binom{j}{ni}\left(\frac{2}{L_1}\right)^{mi}\left(\frac{2}{L_2}\right)^{ni}$$

$$\eta^{2i-mi}\zeta^{j-ni}W_{mi,ni,1}(\eta,\zeta) \tag{20}$$

with

$$W_{m,n,k}(\eta,\zeta) = \int\int_{(r,\varphi)} \cos^m\varphi\sin^n\varphi r^{m+n}S_k(r)drd\varphi \tag{21}$$

Table 1(*a*) Expansion coefficient $P_{i,j}$ and the corresponding temperature profile generated by a third-order solution with $L_1 = L_2 = 1.0$

$P_{00} =$ 2.5000e-01	$P_{01} = -2.2896e-01$	$P_{02} =$ 1.0359e-01	$P_{03} = -3.4222e-02$
$P_{04} =$ 8.516e-03	$P_{05} = -8.7643e-03$	$P_{06} = -4.3067e-03$	$P_{20} = -1.0359e-01$
$P_{21} =$ 9.6454e-02	$P_{22} = -5.8112e-16$	$P_{23} = -8.0216e-02$	$P_{24} = -3.0798e-02$
$P_{25} = -3.6243e-03$	$P_{26} =$ 3.3752e-02	$P_{40} = -8.5162e-02$	$P_{41} =$ 5.3491e-02
$P_{42} = -3.0798e-02$	$P_{43} =$ 6.4432e-02	$P_{44} = -5.9828e-16$	$P_{45} = -1.6837e-01$
$P_{46} =$ 1.0463e-01	$P_{60} =$ 4.3067e-03	$P_{61} = -3.7104e-02$	$P_{62} = -3.3752e-02$
$P_{63} =$ 1.3701e-01	$P_{64} = -1.0463e-01$		

ζ \ η	0	0.2	0.4	0.6	0.8	1.0
1.0000	0.0859	0.0848	0.0819	0.0767	0.0661	0.0401
0.8000	0.1151	0.1132	0.1080	0.0997	0.0878	0.0680
0.6000	0.1427	0.1405	0.1339	0.1237	0.1095	0.0891
0.4000	0.1729	0.1702	0.1621	0.1489	0.1304	0.1046
0.2000	0.2081	0.2047	0.1945	0.1775	0.1534	0.1211
0.0000	0.2500	0.2458	0.2332	0.2118	0.1813	0.1422
0.2000	0.3002	0.2953	0.2802	0.2540	0.2159	0.1663
−0.4000	0.3606	0.3551	0.3379	0.3070	0.2591	0.1901
−0.6000	0.4336	0.4280	0.4102	0.3763	0.3181	0.2190
−0.8000	0.5222	0.5175	0.5025	0.4726	0.4122	0.2832
−1.0000	0.6297	0.6278	0.6235	0.6152	0.5828	0.4599

Table 1(*b*) $Q_\eta(\eta,\xi)$ generated from a third-order solution with $L_1 = L_2 = 1.0$

ζ \ η	0	0.1667	0.3333	0.5000	0.6667	0.8333	1.0000
1.0000	0.0000	0.0184	0.0362	0.0528	0.0671	0.0795	0.0894
0.8333	0.0000	0.0229	0.0442	0.0653	0.0845	0.1025	0.1158
0.6667	0.0000	0.0274	0.0539	0.0784	0.1002	0.1234	0.1385
0.5000	0.0000	0.0275	0.0641	0.0961	0.1234	0.1474	0.1651
0.3333	0.0000	0.0371	0.0766	0.1124	0.1433	0.1714	0.1929
0.1667	0.0000	0.0455	0.0905	0.1329	0.1695	0.1996	0.2215
0.0000	0.0000	0.0534	0.1029	0.1527	0.1961	0.2333	0.2588
−0.1667	0.0000	0.0577	0.1163	0.1732	0.2255	0.2687	0.2970
−0.3333	0.0000	0.0593	0.1243	0.1897	0.2496	0.3102	0.3459
−0.5000	0.0000	0.0560	0.1256	0.1996	0.2784	0.3535	0.3984
−0.6667	0.0000	0.0550	0.1152	0.1868	0.2570	0.3889	0.4594
−0.8333	0.0000	0.0417	0.0867	0.1437	0.2271	0.3721	0.5375
−1.0000	0.0000	0.0225	0.0451	0.0686	0.0925	0.1179	0.6436

Table 1(*c*) $Q_\xi(\eta,\xi)$ generated from a third-order solution with $L_1 = L_2 = 1.0$

ζ \ η	0	0.1667	0.3333	0.5000	0.6667	0.8333	1.0000
1.0000	0.2439	0.2435	0.2331	0.2213	0.2055	0.1830	0.1594
0.8333	0.2645	0.2632	0.2533	0.2386	0.2205	0.1974	0.1735
0.6667	0.2907	0.2868	0.2807	0.2613	0.2537	0.2167	0.1873
0.5000	0.3200	0.3163	0.3071	0.2877	0.2659	0.2358	0.2023
0.3333	0.3572	0.3523	0.3408	0.3215	0.2924	0.2582	0.2192
0.1667	0.3992	0.3945	0.3827	0.3625	0.3239	0.2836	0.2378
0.0000	0.4484	0.4443	0.4272	0.3999	0.3614	0.3130	0.2578
−0.1667	0.5059	0.4977	0.4791	0.4459	0.4063	0.3482	0.2787
−0.3333	0.5630	0.5590	0.5416	0.5112	0.4614	0.3892	0.3005
−0.5000	0.6253	0.6225	0.6091	0.5834	0.5311	0.4448	0.3237
−0.6667	0.6828	0.6817	0.6735	0.6631	0.6109	0.5283	0.3469
−0.8333	0.7310	0.7315	0.7349	0.7395	0.7328	0.6719	0.3710
−1.0000	0.7615	0.7621	0.7719	0.7848	0.8034	0.8362	0.8922

$$G_{m,n,k}(x,y) = x^k \int_0^{\tan^{-1}\frac{y}{x}} S_{2+m+n-k}(x\sec\varphi)\tan^m\varphi\cos^{m+n-k}\varphi\, d\varphi \qquad (22)$$

and

$$\eta^+ = \frac{L_1}{2}(1+\eta) \qquad (23)$$

$$\eta^- = \frac{L_1}{2}(1-\eta)$$

$$\zeta^+ = \frac{L_2}{2}(1+\zeta) \qquad (24)$$

$$\zeta^- = \frac{L_2}{2}(1-\zeta)$$

Evaluating equation (19) at $(n+1)(2n+1)$ discrete locations ($\eta = i/n$, $i = 0, \ldots n$; $\zeta = j/n$, $j = -n, \ldots, 0, \ldots n$), a matrix equation is generated for the determination of $P_{2i,j}$.

Once the coefficients $P_{2i,j}$ are determined, the corresponding heat fluxes can be written as

$$Q_\eta(\eta,\zeta) = -\sum_{i=0}^{i=n}\sum_{j=0}^{j=2n} P_{2i,j} NY_{2i,j}(\eta,\zeta,L_1,L_2) + G_{1,0,0}(\zeta^+,\eta^+) - G_{1,0,0}(\zeta^+,\eta^-) \qquad (25)$$

Table 2 Third-order results for the radiative heat flux at the lower wall, $Q_\xi(\eta, -1)$

L_1	L_2	$\eta=0$	0.1667	0.0500	0.8333
0.1	0.1	0.9687	0.9689	0.9712	0.9769
	0.5	0.9624	0.9627	0.9647	0.9697
	1.0	0.9579	0.9582	0.9603	0.9658
	2.0	0.9485	0.9488	0.9514	0.9578
	5.0	0.9310	0.9313	0.9345	0.9421
1.0	0.1	0.9210	0.9213	0.9241	0.9402
	0.5	0.7954	0.7973	0.8137	0.8606
	1.0	0.7615	0.7621	0.7848	0.8362
	2.0	0.7514	0.7537	0.7730	0.8183
	5.0	0.7376	0.7395	0.7561	0.8003
5.0	0.1	0.9158	0.9159	0.9159	0.9273
	0.5	0.7074	0.7081	0.7152	0.7760
	1.0	0.5686	0.5708	0.5924	0.6963
	2.0	0.4476	0.4521	0.4919	0.6350
	5.0	0.3802	0.3859	0.4362	0.5854

Table 3 Third-order results for the radiative heat flux at the upper wall, $Q_\xi[\eta,1)$

L_1	L_2	$\eta=0$	0.1667	0.5000	0.8333
0.1	0.1	0.4153	0.4124	0.3899	0.3484
	0.5	0.0612	0.0611	0.0607	0.0599
	1.0	0.0172	0.0172	0.0171	0.0171
	2.0	0.0021	0.0021	0.0021	0.0021
	5.0	0.0000	0.0000	0.0000	0.0000
1.0	0.1	0.9029	0.9016	0.8849	0.7521
	0.5	0.5178	0.5117	0.4616	0.3585
	1.0	0.2439	0.2435	0.2213	0.1830
	2.0	0.0638	0.0633	0.0596	0.0523
	5.0	0.0000	0.0000	0.0000	0.0000
5.0	0.1	0.9156	0.9155	0.9155	0.8981
	0.5	0.7003	0.6994	0.6877	0.5753
	1.0	0.5356	0.5328	0.5012	0.3657
	2.0	0.3276	0.3230	0.2825	0.1864
	5.0	0.0750	0.0734	0.0614	0.0357

Table 4 Third-order results for the radiative heat flux at the side wall, $Q_\eta(1,\xi)$

L_1	L_2	$\xi=-018333$	-0.3333	0	0.3333	0.8333
0.1	0.1	0.4719	0.3452	0.2767	0.2208	0.1565
	0.5	0.3142	0.0717	0.0356	0.0206	0.0101
	1.0	0.1866	0.0207	0.0090	0.0048	0.0015
	2.0	0.0828	0.0048	0.0018	0.0008	0.0000
	5.0	0.0308	0.0000	0.0000	0.0000	0.0000
1.0	0.1	0.5409	0.4964	0.4704	0.4454	0.4078
	0.5	0.5601	0.4359	0.3694	0.3202	0.2286
	1.0	0.5375	0.3459	0.2588	0.1929	0.1158
	2.0	0.4732	0.2076	0.1233	0.0740	0.0313
	5.0	0.3319	0.0491	0.0165	0.0058	0.0000
5.0	0.1	0.5350	0.4909	0.4660	0.4426	0.4081
	0.5	0.5815	0.4711	0.4136	0.3607	0.2829
	1.0	0.5928	0.4435	0.3689	0.3021	0.2076
	2.0	0.5789	0.3847	0.2959	0.2224	0.1266
	5.0	0.5168	0.2401	0.1526	0.0948	0.0328

Table 5 Third-order results for the centerline temperature $\theta(0,\xi)$

L_1	L_2	$\xi=-1.0$	-0.4	0	0.4	1.0
0.1	0.1	0.5179	0.3329	0.2500	0.1935	0.1373
	0.5	0.5206	0.0959	0.0533	0.0345	0.0189
	1.0	0.5226	0.0405	0.0203	0.0123	0.0050
	2.0	0.5264	0.0125	0.0058	0.0039	0.0005
	5.0	0.5330	0.0000	0.0000	0.0000	0.0000
1.0	0.1	0.5596	0.5093	0.4797	0.4503	0.4016
	0.5	0.6171	0.4544	0.3697	0.2959	0.1927
	1.0	0.6297	0.4336	0.2500	0.1729	0.0859
	2.0	0.6345	0.2205	0.1178	0.0653	0.0219
	5.0	0.6415	0.0601	0.0170	0.0054	0.0000
5.0	0.1	0.5706	0.5257	0.4995	0.4733	0.4284
	0.5	0.6839	0.5636	0.4953	0.4272	0.3083
	1.0	0.7474	0.5782	0.4830	0.3892	0.2292
	2.0	0.7990	0.5626	0.4355	0.3180	0.1363
	5.0	0.8276	0.4134	0.2500	0.1419	0.0306

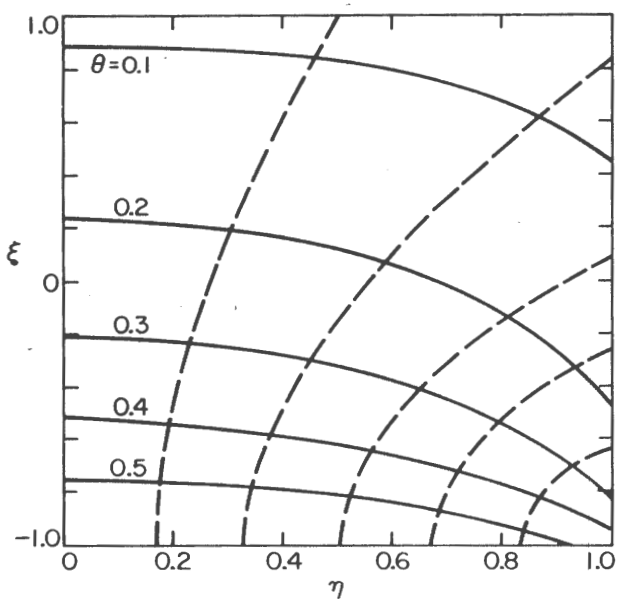

Fig. 5 Isotherms (——) and flux lines (---) for the case with $L_1 = L_2 = 1.0$

$$Q_\zeta(\eta,\zeta) = -\sum_{i=0}^{i=n}\sum_{j=0}^{j=2n} P_{2i,j} NZ_{2i,j}(\eta,\zeta,L_1,L_2) + G_{0,1,0}(\zeta^+,\eta^+) + G_{0,1,0}(\zeta^+,\eta^-) \tag{26}$$

where

$$NY_{2i,j} = \sum_{mi=0}^{mi=2i}\sum_{ni=0}^{ni=j}\binom{2i}{mi}\binom{j}{ni}\left(\frac{2}{L_1}\right)^{mi}\left(\frac{2}{L_2}\right)^{ni} \eta^{2i-mi}\zeta^{j-ni} W_{mi+1,ni,2}(\eta,\zeta) \tag{27}$$

and

$$NZ_{2i,j} = \sum_{mi=0}^{mi=2i}\sum_{ni=0}^{ni=j}\binom{2i}{mi}\binom{j}{ni}\left(\frac{2}{L_1}\right)^{mi}\left(\frac{2}{L_2}\right)^{ni} \eta^{2i-mi}\zeta^{j-ni} W_{mi,ni+1,2}(\eta,\zeta) \tag{28}$$

It is important to note that based on the mathematical properties of $S_n(x)$ developed in [8], a set of recursive relations for $G_{m,n,k}(\eta,\zeta)$ and $W_{m,n,k}(\eta,\zeta)$ can be readily generated. They are listed in Appendix A. Based on these relations, $M_{2i,j}$, $NY_{2i,j}$ and $NZ_{2i,j}$ in the above equations can be readily evaluated. Indeed, the analysis in Appendix A shows that the present technique requires only the numerical evaluation of a finite number of single integrals for a complete solution to the problem.

4 Results and Discussion

(a) Numerical Accuracy and Efficiency. The major advantage of the present solution method is that extremely accurate solutions for both the temperature and heat flux distribution can be readily obtained with little effort. Predictions of the centerline temperature and heat flux distribution at the bottom walls generated by the first three approximation ($n = 1,2,3$) of the present approach and those obtained by the Hottel zonal method as reported in [4] are compared in Figs. 3 and 4. The rapid rate of convergence shown in those figures holds in general for all optical thicknesses L_1 and L_2.

Direct comparison between different numerical procedures based on computer time is difficult and often misleading because computer time depends not only on the complexity of the calculation, but also on the size of a computer and the

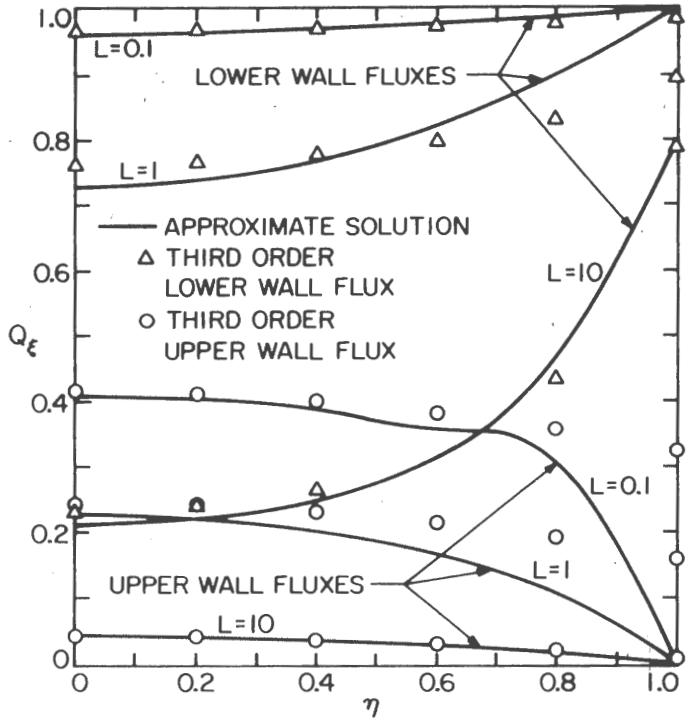

Fig. 6 Comparison between equation (30) and the third-order result at the upper and lower wall for enclosures with $L_1 = L_2 = L$

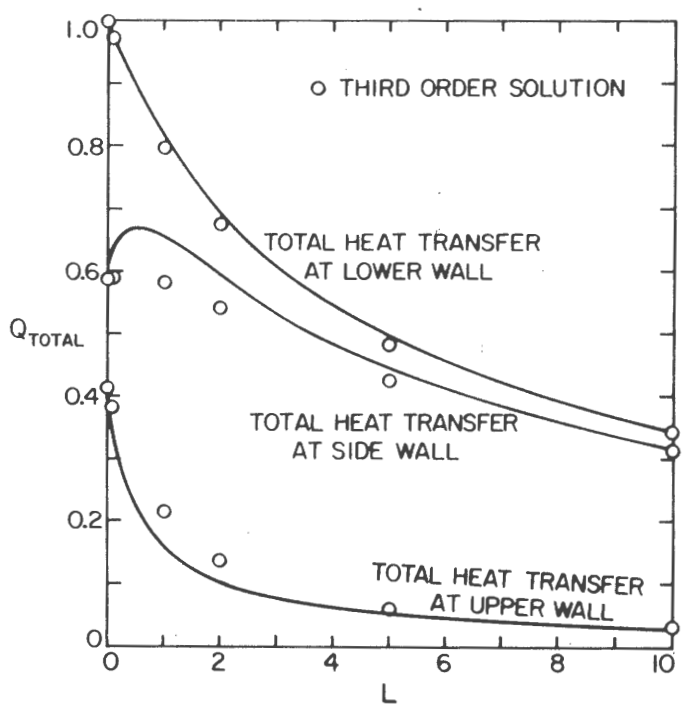

Fig. 7 Comparison between total heat transfer results generated from equation (30) and the corresponding third-order results for enclosures with $L_1 = L_2 = L$

efficiency of the programmer. A more accurate comparison of the relative efficiency between the present technique and the Hottel zonal method is the number of numerical integrals required by the two methods and the relative complexity of the required integrations. Based on results presented in Appendix A, the number of single integration required by the present technique is approximately the same as the number of double integrals required by the Hottel zonal method with the same number of unknowns. Since numerical evaluation of a double integration is at least one order of magnitude more

complex than that of a single integration, the present technique is clearly numerically more efficient than the Hottel zonal method.

Another advantage of the present technique is that in addition to temperature distribution, detailed information concerning heat flux distribution is also generated by the computation with no additional effort. The third-order results of $P_{2i,j}$, $\vartheta(\eta,\zeta)$, $Q_\eta(\eta,\zeta)$ and $Q_\zeta(\eta,\zeta)$ for the case with $L_1=L_2=1$ are presented in Tables 1(*a*), 1(*b*), and 1(*c*). Results in these tables can be combined to yield the isotherm and flux line plot shown in Fig. 5. Similar results for other typical cases (L_1, $L_2=0.1$, 0.5, 1.0, 2.0, 5.0, 10.0) are presented in [10]. Centerline temperature and heat flux distribution at the three boundaries for some typical cases (which might be of interest to researchers for comparison with other techniques) are presented in Tables 2–5. It is interesting to note that to generate the same information based on the Hottel zonal method would require a tripling of the number of double integrations. A direct comparison of numerical results also shows that a 28-zones Hottel zonal calculation is generally less accurate than the present third order solution. To the best of the present authors' knowlege, no other solution methods (approximate or exact) for radiative transfer can generate as much information with such numerical efficiency as the present technique.

(*b*) Important Physical Results. The qualitative behavior of the heat flux and temperature distribution of the present two-dimensional problem is well known from previous studies [1–5]. Results presented in Tables 2–5 demonstrate the expected behavior more quantitatively over a wide range of system parameters.

Over the years, numerous analysis of different engineering systems have been presented in which the radiative heat flux is approximated as a simple diffusion process with $\mathbf{Q}=-4/3\nabla\vartheta$. Until now, quantitative evaluation of the accuracy of this assumption has never been made, except for one-dimensional systems. The isothermal and flux line plot generated by the present work as shown in Fig. 5 offers an interesting possibility for such evaluation. Note that for $L_2=L_1=1$ (which is optically thick compared to most combustion systems), the isothermal line is in not perpendicular to the flux line. The diffusion approximation is thus in general not accurate for such systems, both in predicting the magnitude and the direction of the radiative heat flux vector. The validity of many previous analysis which utilized this approximation is thus needed to be reevaluated. It is also interesting to observe that because of the temperature slip, the isotherms shown in Fig. 5 are not parallel to the isothermal wall.

(*c*) Approximate Solutions. For practical engineering application, the development of accurate and simple-to-use expressions for the prediction of heat transfer and temperature profile within a multidimensional systems at radiative equilibrium is important. Until now, development of such expressions, even empirically, is difficult due to the lack of reliable numerical data. The present results, which include detail information concerning both temperature and heat flux distribution, serve ideally as basis for such development.

In one-dimensional analysis, it is well known [9] that the traditional diffusion approximation is quite accurate and yields the following expression for the radiative heat flux,

$$Q=\frac{1}{1+3L/4} \tag{29}$$

Using the fact that $1/L$ and 1 can be interpreted as the optically thick and thin limits of the radiative heat flux, the present work proposes to generalize the above expression for multidimensional application to become

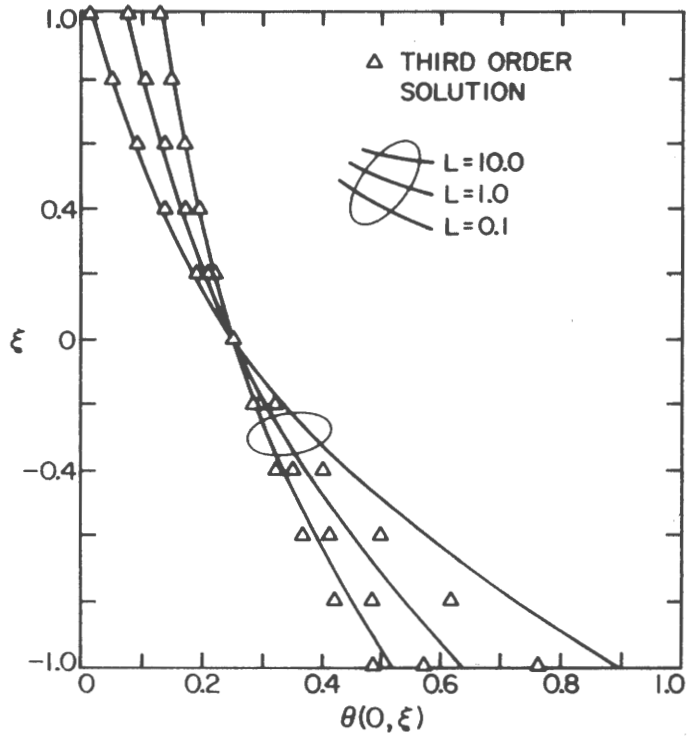

Fig. 8 Comparison between equation (31) and the corresponding third-order solution of the centerline temperature $\theta[0,\xi)$ with $L_1=L_2=L$

$$Q_i=\frac{1}{\dfrac{1}{Q_{0,i}}+\dfrac{3}{4Q_{c,i}}} \qquad i=x,y,z \tag{30}$$

In the above expression, $Q_{0,i}$ stands for the optically thin limiting expression of the radiative heat flux which is a function only of geometry, and $Q_{c,i}$ stands for the corresponding optically thick limit which can be readily generated by solving an equivalent conduction problem with identical boundary conditions. Since solutions to conduction problems (by both analytical and numerical method) are well known, equation (28) clearly represents an exceedingly simplified approach in evaluating approximately radiative heat flux in a multidimensional system.

It is important to note that equation (30) is developed entirely empirically from physical reasoning. It is intended only to be a tool for practicing engineer to generate first-order estimate of the radiative heat flux. For the present rectangular enclosure, however, the accuracy of the expression is surprisingly good. Heat flux distributions and average heat flux at the three boundaries predicted by equation (30) and the corresponding third-order results for different system parameters are compared in Figs. 6 and 7.

Utilizing a similar argument, the present work proposes the following empirical expression for the temperature distribution

$$\vartheta=\left(1-\frac{|\mathbf{Q}|}{|\mathbf{Q}_0|}\right)\vartheta_c+\frac{|\mathbf{Q}|}{|\mathbf{Q}_0|}\vartheta_0 \tag{31}$$

In the above expression, ϑ_c and ϑ_0 stand of the optically thick and thin limiting expression of the medium's temperature, respectively. For a general enclosure, ϑ_0 can be generated by solving an energy equation such as equation (13) in the optically thin limit. For the rectangular enclosure, for example, it can be readily shown that ϑ_0 is given by

$$\vartheta_0(\eta,\zeta)=\frac{1}{4\pi}(\varphi_2-\varphi_1) \tag{32}$$

Similar to $\mathbf{Q}_c(\eta,\zeta)$, $\vartheta_c(\eta,\zeta)$ can be generated from an analytical or numerical solution to a corresponding con-

duction problem. The accuracy of equation (31) is again quite good for the rectangular enclosure. Centerline temperature profiles generated by equation (31) and the corresponding third-order results for some typical cases are shown in Fig. 8.

5 Conclusion

Radiative heat transfer in a rectangular enclosure with gray medium at equilibrium is considered. The method of point allocation is demonstrated to be effective in generating accurate solutions to the problem. Utilizing properties of $S_n(x)$, a class of generalized exponential integral functions studied extensively in a previous reference [8], the present solution technique is shown to be extremely efficient compared to the Hottel zonal method. Detailed temperature and heat flux distribution both within the medium and at the different boundaries are readily generated from the present approach. Based on the present results, the physics of multidimensional radiative heat transfer is illustrated and discussed.

Simple closed-form expressions are proposed for the estimate of heat transfer and temperature profile in a multidimensional system at radiative equilibrium. These expressions are generated empirically by requiring that they have the correct behavior in both the optically thick and thin limits and are intended only for practical engineering application. For the rectangular enclosure, the accuracy of these expressions over all optical thicknesses is demonstrated to be good.

6 Acknowledgment

This work is based upon work supported by the National Science Foundation Grants No. ENG 78-05587 and MEA 80-24824.

References

1 Taniguchi, H., "The Radiative Heat Transfer of Gas in a Three-Dimensional System Calculated by Monte Carlo Method," *Bulletin JSME*, Vol. 12, 1969, pp. 67–78.

2 Hottel, H. C., and Cohen, E. S., "Radiant Heat Exchange in a Gas-Filled Enclosure: Allowance for Non-Uniformity of Gas Temperature," *AIChE Journal*, Vol. 4, No. 1, 1958, pp. 3–14.

3 Glatt, L., and Olfe, D. B., "Radiative Equilibrium of a Gray Medium in a Rectangular Enclosure," *Journal of Quantitative Spectroscopy and Radiative Transfer*, Vol. 13, 1973, pp. 881–895.

4 Modest, M. F., "Radiative Equilibrium of a Gray Medium in a Rectangular Enclosure," *Journal of Quantitative Spectroscopy and Radiative Transfer*, Vol. 15, 1975, pp. 445–461.

5 Modest, M. F., "Two-Dimensional Radiative Equilibrium of a Gray Medium Between Concentric Cylinders," *Journal of Quantitative Spectroscopy and Radiative Transfer*, Vol. 19, 1978, pp. 353–365.

6 Yuen, W. W., and Tien, C. L., "A Successive Approximation Approach to Problems in Radiative Transfer with a Differential Formulation," ASME JOURNAL OF HEAT TRANSFER, Vol. 102, No. 1, 1980, pp. 86–91.

7 Yuen, W. W., and Wong, L. W., "Heat Transfer by Conduction and Radiation in a One-Dimensional Absorbing, Emitting and Anisotropically Scattering Medium," ASME JOURNAL OF HEAT TRANSFER, Vol. 102, 1980, pp. 303–307.

8 Yuen, W. W., and Wong, L. W., "Numerical Computation of an Important Integral Function in Two-Dimensional Radiative Transfer," *Journal of Quantitative Spectroscopy and Radiative Transfer*, Vol. 29, No. 2, 1983, pp. 145–149.

9 Siegel, R., and Howell, J. R., *Thermal Radiation Heat Transfer*, McGraw-Hill, N.Y., 1972.

10 Yuen, W. W., "Numerical Results of Radiative Heat Transfer in a Rectangular Enclosure With Gray Medium at Radiative Equilibrium," UCSB Report No. ME-83-1, 1983.

APPENDIX A

Properties of $W_{m,n,k}(\eta,\varphi)$ and $G_{m,n,k}(x,y)$

Using the recursive relation of $S_n(x)$ as illustrated in [8], it can be readily shown that

$$\int_0^r S_k(x)x^{m+n}dx=(m+n)!\left[S_{m+n+k+1}(0)-\sum_{s=0}^{s=m+n}S_{m+n+k+1-s}(r)\frac{r^s}{s!}\right] \tag{A1}$$

Based on the above equation, equation (21) is reduced to

$$W_{m,n,k}(\eta,\varphi)=-(m+n)!\left[\sum_{s=0}^{s=m+n}\frac{H_{m,n,k,s}(\eta,\varphi)}{s!}-\frac{[1+(-1)^m][1+(-1)^n]}{2}\left[\frac{\Gamma\left(\frac{m+1}{2}\right)\Gamma\left(\frac{n+1}{2}\right)}{\Gamma\left(\frac{m+n+2}{2}\right)}\right]S_{m+n+k+1}(0)\right] \tag{A2}$$

where

$$H_{m,n,k,s}(\eta,\varphi)=\int_0^{2\pi}[r(\varphi)]^s S_{m+n+k+1-s}[r(\varphi)]\cos^m\varphi\sin^n\varphi d\varphi \tag{A3}$$

Values for $r(\varphi)$ can be readily deduced from Fig. 2. Indeed, $H_{m,n,1,s}(\eta,\varphi)$, which is required for the solution to equation (19), can be expressed as

$$\begin{aligned}H_{m,n,1,s}(\eta,\varphi)=&G_{n,m,s}(\eta^-,\zeta^-)+G_{m,n,s}(\zeta^-,\eta^-)\\&(-1)^m[G_{n,m,s}(\eta^+,\zeta^-)+G_{m,n,s}(\zeta^-,\eta^+)]\\&(-1)^n[G_{n,m,s}(\eta^-,\zeta^+)+G_{m,n,s}(\zeta^+,\eta^-)]\\&(-1)^{m+n}[G_{n,m,s}(\eta^+,\zeta^+)+G_{m,n,s}(\zeta^+,\eta^+)]\end{aligned} \tag{A4}$$

where η^+, η^-, ζ^+, and ζ^- are as defined by equations (23) and (24). Similar expressions can also be generated for $H_{m,n,2,s}(\eta,\zeta)$, which is required for the evaluation of heat fluxes.

The foregoing development proves that the evaluation of $W_{m,n,1}(\eta,\varphi)$ and $W_{m,n,2}(\eta,\varphi)$ requires only the evaluation of $G_{m,n,k}(x,y)$. Based on equation (22) and properties of $S_n(x)$, it can be readily shown that $G_{m,n,k}(x,y)$ satisfies

$$G_{m,n,k}(x,y)=\begin{cases}x^kG_{m,n-k,0}(x,y) & k<n\\ x^nG_{m,0,k-n}(x,Y) & n<k<m+n\end{cases} \tag{A5}$$

and

$$G_{m,n,0}(x,y)=-\frac{S_{2+m+n}[(x^2+y^2)^{1/2}]y^{m-1}x^{n+1}}{(1+n)[(x^2+y^2)^{1/2}]^{m+n}}+\frac{(m-1)G_{m-2,n+2,0}(x,y)-xG_{m,n-1,0}(x,y)}{1+n} \tag{A6}$$

when $m>1$ and $n>1$ and

$$G_{m,0,k}(x,y)=-\frac{S_{3+m-k}[(x^2+y^2)^{1/2}]xy^{m-1}}{[(x^2+y^2)^{1/2}]^{m-k+1}}+(k-2)G_{m,0,k-1}(x,y)+(m-1)x^2G_{m-2,0,k-3}(x,y) \tag{A7}$$

when $k>2$.

Based on the foregoing relations, it is apparent that the determination of $G_{m,n,k}(x,y)$ requires only the numerical evaluation of $G_{m,0,0}(x,y)$, $G_{0,n,0}(x,y)$, $G_{m,0,1}(x,y)$ and $G_{m,0,2}(x,y)$. In the Nth approximation, the value of m and n required for the evaluation of various coefficients in equations (19), (25), and (26) ranges between 0 and $2N+1$. At each allocation point, each integral is required to be evaluated 4 times (for both η^+, η^-, and ζ^+, ζ^-). For $(2N+1)(N+1)$ allocation points, a total of $16(2N+2)(2N+1)(N+1)$ single integrations are thus required for the Nth order solution. A Hottel zonal calculation utilizing $(2N+1)(N+1)$ zones, on the other hand, would require a total of $(2N+1)(N+1)[(2N+1)(N+1)+1]/2$ double integrations.